Delft University of Technology

Reliability analysis of reinforced concrete vehicle bridges columns using non-parametric Bayesian networks

Mendoza Lugo, M.A.; Delgado-Hernández, David-Joaquín; Morales Napoles, Oswaldo

DOI
10.1016/j.engstruct.2019.03.011

Publication date
2019

Document Version
Accepted author manuscript

Published in
Engineering Structures

Citation (APA)
Mendoza Lugo, M. A., Delgado-Hernández, D.-J., & Morales Napoles, O. (2019). Reliability analysis of reinforced concrete vehicle bridges columns using non-parametric Bayesian networks. *Engineering Structures*, *188*, 178-187. https://doi.org/10.1016/j.engstruct.2019.03.011

Important note
To cite this publication, please use the final published version (if applicable).
Please check the document version above.

Copyright
Other than for strictly personal use, it is not permitted to download, forward or distribute the text or part of it, without the consent of the author(s) and/or copyright holder(s), unless the work is under an open content license such as Creative Commons.

Takedown policy
Please contact us and provide details if you believe this document breaches copyrights.
We will remove access to the work immediately and investigate your claim.

This work is downloaded from Delft University of Technology.
For technical reasons the number of authors shown on this cover page is limited to a maximum of 10.

© 2018 Manuscript version made available under CC-BY-NC-ND 4.0 license
https://creativecommons.org/licenses/by-nc-nd/4.0/

Reliability analysis of reinforced concrete vehicle bridges columns using non-parametric Bayesian networks[☆]

Miguel Angel Mendoza-Lugo[a,1,*], David Joaquin Delgado-Hernandez[c,2,**], Oswaldo Morales-Napoles[b,3]

[a] *Cerro de Coatepec, Ciudad Universitaria,50100,Toluca, Mexico*
[b] *Cerro de Coatepec, Ciudad Universitaria,50100,Toluca, Mexico*
[c] *Postbus 5, 2600AA, Delft, The Netherlands*

Abstract

In the bridge industry, current traffic trends have increased the likelihood of having the simultaneous presence of both extreme live loads and earthquake events. To date, their concurrent interaction has scarcely been systematically studied. Prevailing studies have investigated the isolated existence of either live loads or seismic actions.

In an effort to fill this gap in the literature, a non-parametric Bayesian Network (BN) has been proposed. It is aimed at evaluating the conditional probability of failure for a reinforced concrete bridge column, subject simultaneously to the actions mentioned above. Based on actual data from a structure located in the State of Mexico, a Monte Carlo Simulation model was developed. This led to the construction of a BN with 17 variables.

The set of variables included in the model can be categorized into three groups: acting loads, materials resistances and structure force-displacement behavior. Practitioners are then provided with a tool for unspecialized labor force to gather information in-situ (e.g. Weight-In-Motion data and Schmidt hammer measurements), which can be included in the network, leading to an updated probability of failure. Moreover, this framework also serves as a quantitative tool for bridge column reliability assessments.

[☆] This document is a collaborative effort.

[*] Corresponding author
[**] Principal corresponding author
Email addresses: mamendozal@uaemex.mx (Miguel Angel Mendoza-Lugo), delgadoh01@yahoo.com (David Joaquin Delgado-Hernandez), o.moralesnapoles@tudelft.nl (Oswaldo Morales-Napoles)
[1] Autonomous University of the State of Mexico.
[2] Autonomous University of the State of Mexico.
[3] Delft University of Technology.

Results from the theoretical model confirmed that the bridge column probability of failure was within the expected range reported in the literature. This reflects not only the appropriateness of its design but also the suitability of the proposed BN for reliability analysis.

Keywords: `Bridge`, Reliability, Reinforced concrete columns, Bayesian Networks
2010 MSC: 00-01, 99-00

---

1. Introduction.

Bridges are high impact engineering structures which are menaced by different hazards such as earthquakes and high traffic loads. Then the possibility of having the combined presence of live loads and seismic events is not remote [1]. These events may lead to a bridge damage which in turn may provoke negative consequences in the transportation systems.

Vehicle loads exceeding the legal weight limits, cause serious threats to road transport operations. Live-load models of many codes of practice are theoretical only, and are commonly calibrated for reproducing a load effect and not the actual magnitude of the load itself [2]. Additionally the frequent occurrence of earthquakes could lead to damage and would further accelerate the deterioration of bridges, which might conduce eventually to a catastrophic failure. [3].

In order to assess the impacts of the previously described scenario, reliability analyses are performed. To do so, it is necessary to gather consistent measures of safety under uncertain events. Among the available reliability tools, Bayesian Networks (BN's) offer the opportunity to fulfill these requirements, because they represent multidimensional probability problems with a reduced number of parameters. In addition, BN's can be updated when new data becomes available.

The purpose of this piece of research is to estimate the bridge reinforced concrete column conditional Probability of Failure (POF) through a BN. To this end, the variables considered in the study are: seismic intensity, traffic loads and materials properties. The main originality of this paper consists in the possibility of updating such POF by considering new practical information.

In the subsequent sections, a typical Mexican bridge will be firstly presented. Then, the failure mechanisms of RC columns will be explained. Next, the theory behind BN's will be discussed in combination with the variables considered in the research. To complete the discussion, some limit state functions will be introduced. Then, the resultant BN and its main features will be explained, along with its use in the above mentioned structure. The main findings of the study will then be discussed. Finally, the conclusions of the investigation will be drawn.

2. Mexican bridge

The structural element under analysis is the central bent column of a bridge built in 2014, with two lanes and located in the state of Mexico. The bridge has eight 35.0 m spans, each of which has six concrete box girders. Their ends rest on bents composed by 2 circular RC columns, with a diameter of 1.40 m and a square pier cap of 1.4 m. The length and cross section of the interest column are depicted in Figure 1. In terms of its reinforcement features, 37 longitudinal steel bars with a diameter of 25.4 mm, and spiral transversal reinforced with 12.7 mm steel bar (1 turn every 10 cm) are considered.

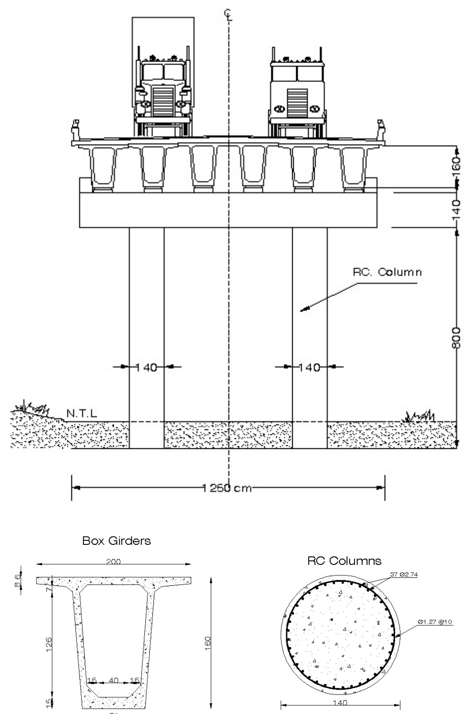

Figure 1: Plane, vertical view and details of the structure under analysis [cm].

The bridge under study was chosen because it represents 73.1% of the structures built in the state of Mexico [4] over the last four decades. Moreover, it is situated in a seismic zone with frequent annual activity [5]. In parallel, considerable traffic loads use the structure on a daily basis [6]. Consequently, it fulfilled the established criteria to carry out the required analysis. Prior to explaining the construction of the BN, it is important to understand the RC column failure modes.

3. Reinforced concrete columns failures modes

There are different failure mechanisms of RC columns, e.g. structural instability and pure compression. The recorded data of damaged columns during past strong motion events revealed two main failure conditions: flexural and shear [7]. As will be discussed later, these two have been chosen to propose the limit state functions to perform a reliability analysis. Moreover, to include a service limit state evaluation, the drift exceed likelihood of the element will also be assessed. Even though a comprehensive description of the failure modes can be found elsewhere [8], next some highlights will be presented.

3.1. Combined axial and flexural strength

Interaction diagrams are a visual representation of the combined loads, usually bending moment (M) and axial load (P), that will cause the RC column to fail. These diagrams are created assuming a series of strain distributions and computing the corresponding values of P and M [9]. Following the steps detailed in [10], the nominal axial load (P) and the bending moment capacity (M) about the assumed neutral axis were estimated the for element of interest.

3.2. Shear strength

The shear strength (V_U) of RC members is affected by a number of parameters: applied shear stress level, level of imposed ductility, level of axial compression force, aspect ratio, transverse steel ratio, and longitudinal steel ratio [11]. V_U for a circular cross section in combined bending and compression stress regime adopted in the Mexican code NTC RCDF[12] is given as follows:

$$V_U = V_{CR} + V_{SR} \tag{1}$$

Where V_{CR} is the contribution of the concrete to shear strength, and V_{SR} is the contribution of the shear reinforcement.

3.3. Drift

Since this research is aimed at obtaining the POF of the mentioned limit states, the resistance component in this case will be the permissible drift. Basically, the drift (γ) is a representative measure of a structural system affected by seismic forces, calculated as:

$$\gamma = \frac{U}{H} \tag{2}$$

Where H is the height of the column and U is the lateral displacement.

Based on the recommendations given in [13], a response modification factor (R=3) for vertical RC vertical piles was selected. According to the Mexican procedure NTC-RSEE [14], the corresponding maximum drift value is γ_{max}=0.02. Having highlighted these points, in the next section the theory behind BN's will be briefly presented.

4. Non-Parametric Bayesian Networks

The literature reports various studies within the reliability bridge analysis, centered on the use of fuzzy logic [15], the analytic hierarchy process [16] and fragility curves [17]. Another tool that could be used in the exercise is a BN. Based on the discussion reported in [18], which highlights the advantages of using BNs in the bridge industry, such a tool has been adopted here. Bayesian Networks are directed acyclic graphs, consisting of nodes and arcs. The first represent uncertain or random variables which can be either continuous, discrete or functional. And the latter represent the causal or influential links between these uncertain variables [19].

The theory of non-parametric BN's is built around bivariate copulas. They are a class of bivariate distributions whose marginals are uniform on the uniform interval [20]. The use of the normal copula reduces and simplifies the joint distribution sampling, when dealing with high dimensional continuous BN's. Correlation = 0 implies independence, for the normal copula. The relationship between the rank correlation of the normal variables r, and the product-moment correlation of the normal variables ρ is given by [21]:

$$\rho(X,Y) = 2sin\left(\frac{\pi}{6}r(X,Y)\right) \tag{3}$$

When building a non-parametric BN, there are two properties that should be validated: (i) that the data has a normal copula and (ii) that the BN represents enough dependence. To do so, the d-calibration score is computed. It uses the following of three variants.

- ERC: empirical rank correlation matrix.
- NRC: empirical rank correlation matrix under the assumption of the normal copula.
- BNRC: Bayesian network rank correlation matrix.

The score is 1 if the matrices are equal, and 0 if one matrix contains a pair of variables perfectly correlated. The score will be "small" as the matrices differ from each other element-wise [22]. The d-calibration score is given by:

$$d(\Sigma_1, \Sigma_2) = 1 - \sqrt{1 - \eta(\Sigma_1, \Sigma_2)} \tag{4}$$

$$\eta(\Sigma_1, \Sigma_2) = \frac{det(\Sigma_1)^{1/4} det(\Sigma_2)^{1/4}}{det\left(\frac{1}{2}\Sigma_1 + \frac{1}{2}\Sigma_2\right)^{1/2}} \tag{5}$$

Where Σ_1 and Σ_2 are the correlation matrices of interest. More details for non parametric BN's can be consulted in [23], [24] and [25]. Now that a typical Mexican bridge has been presented, the failure modes of the RC column discussed, and the BN theory briefly described, the steps for building the network of interest will be exposed.

5. Framework for building the BN

The requirements of the BN have been divided into three categories: traffic loads, ground motion and bridge information. The first refers to the position of the two trucks in the bridge relative to the beginning of the structure, the number of axles per lane, the gross weight per vehicle and the weight per lane. While the length of the bridge span was able to hold up to two vehicles per lane, only one was taken into consideration. This was because of the restriction imposed by the maximum truck legal length [26]. The second considers the seismic accelerograms used in the study with their corresponding Peak Ground Accelerations (PGAs). The third is related to resistance material properties (concrete and reinforcement steel) and the Finite Element Model (FEM) of the bridge.

It should be noted, that the list of variables selected is not exhaustive, it only considered those that take part in the initial stages of the phenomena. The main selection criteria used was the availability of data by means of either experiments, experts or simulation. Figure 2 shows the whole framework for building the BN, based on the model described in [2].

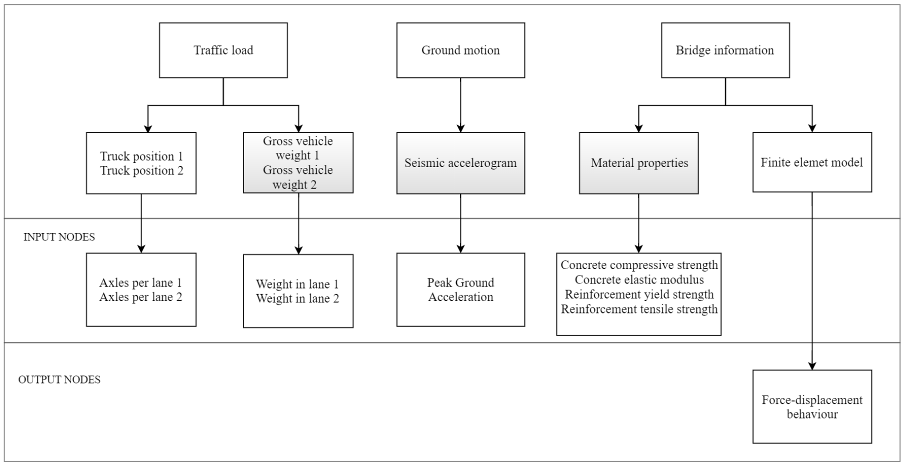

Figure 2: Framework for the joint live load and earthquake loads

To operationalize the process, a computer script was written in MATLAB®, aimed at controlling SAP2000® through an Application Program Interface (API). Bear in mind that a useful method to assess infrastructure performance is Monte Carlo Simulation (MCS), which makes use of random numbers to compute complex phenomena. Basically, random variables with specific distributions can be modeled [27].

The algorithm used to run the exercise included the following phases:

1. For each of the input variables, random numbers are generated via MCS (see input nodes in Figure 2).

2. The MATLAB® script is then executed with the random data.

3. The corresponding output variables are obtained by means of SAP2000®.

4. The processes is repeated.

Here, given the limited computational resources and time to carry out the research, only 3500 realizations have been performed. Each one took approximately two hours to complete. The simulations were run on a personal computer with 64-bit, Windows 10 OS, 8 GB RAM and i7-6700 Intel 3.40 Ghz processor. Nevertheless, it is important to note that the resultant imprecision level is 0.010 for a 99% confidence interval [28]. With these ideas in mind, now the categories within the framework will be detailed.

5.1. Traffic loads

According to the Mexican standard NOM-012-SCT-2-2014 [26] there are three main types of design vehicles with a maximum weight of 740.4 kN. However, empirical evidence has revealed that it is lower than the actual Mexican highway traffic loads. Garcia-Soto [29] reported a maximum gross vehicular weight of 1307.7 kN in a main highway located in central Mexico, i.e. 1.75 times the maximum allowed within the standard.

In terms of the vehicle masses, the weight in motion (WIM) system was designed for quantifying axle loads, vehicular weights, inter axial separations, vehicle lengths and speeds [30]. It represents a good alternative for knowing the traffic flow characteristics in the bridge under analysis. However, evidence about the existence of WIM in Mexico is scarce [29].

As a consequence, and based on the experience of one of the authors [30], who developed a large-scale hybrid BN for traffic load modeling from the WIM system of The Netherlands. Then data from the Dutch WIM was used to carry out the simulation exercise presented in this paper. It should be noted here, that the aim of the research is to establish a theoretical methodology for reliability analysis of RC bridge columns. In a practical evaluation, actual data form the structure under analysis should be employed. Having clarified the point, Figure 3 shows the total truck weight per lane considered for the case study.

As can be seen, the corresponding empirical distribution has a mean of 545 kN, with a standard deviation of 260 kN. Its maximum value is 1464 kN, a quantity comparable with that registered in central Mexico for a single heavy truck [29]. In the next section the ground motion variable will be presented.

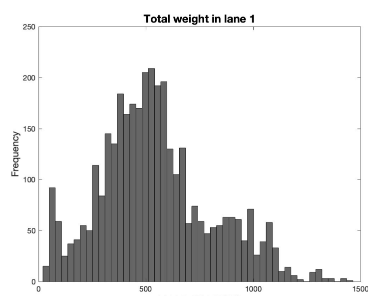

Figure 3: Total weight per lane (one nine axles vehicle).

5.2. Ground motion

Unlike the previous variable, which was easy to operationalize, the ground motion can be represented in different manners. Note that the dynamic characteristics of the bridge have been neglected in this study. Thus, further research should address this limitation. Under these circumstances, according to [31] the most widely used parameter in strong-motion studies is the peak ground acceleration (PGA). Essentially, it has been deemed superior compared to several intensity measures such as: peak ground velocity, peak ground displacement, spectral acceleration, Arias intensity, velocity intensity, cumulative absolute velocity and cumulative absolute displacement. Then, on the basis of efficiency, practicality, proficiency, sufficiency, and hazard computability, PGA is the optimal intensity measure [32].

Once the PGA was selected, to choose the ground motion accelerograms for this study, three alternatives were explored. Being an academic exercise, the goal was to find some earthquakes able to reach the inelastic response of the structure.

1. The Mexican large seismic data base was consulted first [33]. In the event, 98 ground motions with Mw>6, ranging from 1964 to 2018, were identified. Having carried out the structural analysis, the inelastic state of the bridge was not reached.

2. The seismic design program (PRODISIS) [34] developed by the Mexican Federal Electricity Commission (CFE) was now used. It allowed the generation of 100 synthetic accelerograms in the bridge location. These were used in the structural analysis. Once again, the inelastic state of the structure was not reached.

3. The ground motion database proposed by Caltrans engineers from the Pacific Earthquake Engineering Research Center, was then chosen [35]. Specifically, it was utilized in [36] in a probabilistic seismic demand analysis. In this case, the inelastic state of the bridge was finally reached.

Consequently, 12 three-components (longitudinal, transverse, and vertical) ground motions were selected from the latter. To complement the database, the no-earthquake scenario and the ground motion occurred on 2017-09-19 in Mexico was also included, leading to a total of 14 records. The 2017 earthquake was elected not only for its epicenter location (about 100 km away from the bridge), but also for the need to include at least one Mexican record in the analysis. These ground motions cover low, moderate, and high hazard seismic levels, as shown in Table 1.

Table 1: General characteristics of the ground motions.

Earthquake	Year	Station	PGA
No-earthquake	–	–	0.000
Morelos, MX	2017	DX37	0.191
Livermore, USA	1989	MGNP	0.245
Morgan Hill, USA	1984	CCLYD	0.273
Loma Prieta,USA	1989	LEX	0.403
Loma Prieta,USA	1989	GILB	0.447
Coyote Lake,USA	1979	CLYD	0.527
Parkfield,USA	1966	CS050	0.659
Loma Prieta, USA	1989	GAV	0.695
Loma Prieta, USA	1989	LGPC	0.783
Kobe, JP	1995	KOB	0.824
Tottori,JP	2000	TTR	0.975
Northridge, USA	1989	COR	1.026

The years of the events range from 1966 to 2017. While nine of them were recorded in the USA, two were registered in Japan and one in Mexico. Since all of them led to damage of RC bridge columns either by flexural or shear stresses [7], they were considered in the current research. Strictly speaking, only the Mexican record should be used in the assessment of the structure analyzed. Nevertheless, the use of the other ground motions helps to better understand the phenomena under study. Now that the first two categories of the framework have been established, the third will be presented.

5.3. Bridge information

The Mexican bridge has already been described in terms of its geometry and reinforcement features (see Figure 1 above). To enhance the description, both its material properties and its finite element model will next be described.

5.3.1. Material properties

Four mechanical properties were introduced into the BN: concrete compressive strength ($f'c$), concrete elastic modulus (E_c), reinforced steel yield strength (fy) and tensile strength (f_u). These variables were chosen because they are required in the in-situ tests established in the Mexican standards [12], [37], [38], [39], [40], [41], [42] and [43]. The empirical part of the research consisted of collecting data from 64 fresh concrete cylindrical specimens, and 44 representative longitudinal reinforcement samples. They were obtained during the bridge construction process.

Given the results of the laboratory test, the model uncertainties for resistance have been considered as random variables. They are described by appropriate probability density functions (pdfs). The type of distribution and the relevant statistical parameters found in the case study are listed in Table 2

Table 2: Random variables, type of distribution and parameters found in the case study.

Random Variable	Distribution	μ	σ
$f'c(MPa)$	Lognormal	3.4782	0.10988
$E_c(MPa)$	Lognormal	10.181	0.061225
$f_y(MPa)$	Lognormal	6.1321	0.080797
$f_u(MPa)$	Normal	7.1614	46.498

Due to the scarcity of field data, dependence models such as the gaussian copula can be employed to generate random data having the statistical characteristics of the specimens. Thereby, given the correlation between $f'c - Ec$ and $fy - fu$, a random gaussian copula is generated. First the Pearson's coefficient (ρ) is computed using a small sample of empirical data (see Figure 4a). Through equation (3) the associated Spearman's rank (r) is calculated (see Figure 4b). This enables to generate a larger sample of data based on the original data source.

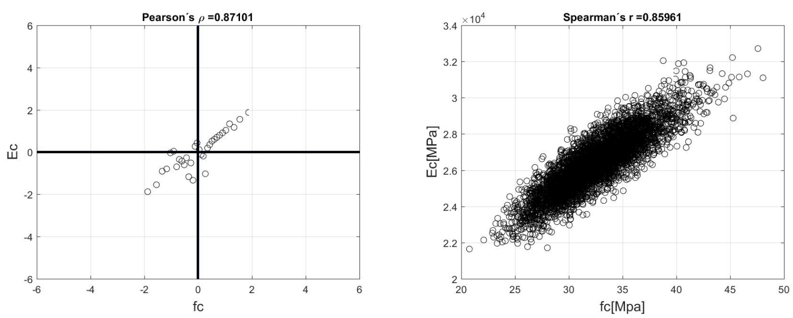

(a) $f'c - Ec$ copula

(b) $f'c - Ec$ scatter plot

Figure 4: $f'c - Ec$ copula and scatter plot.

Once the random pair sample is computed, each material property is entered into the finite element model, which will now be described.

5.3.2. Finite element model

The numerical model is aimed at understanding the bridge behavior. The variables of interest here include: maximum axial load (MaxP), maximum shear (MaxV), maximum bending moment (MaxM), and lateral displacements (U). A simplified FEM of the structure has been built using SAP2000 v.14 bridge wizard module [44]. Following the guidelines for non-linear analysis of bridge structures [35], the subsequent assumptions are considered:

- Three component ground motion non-linear time history analysis is executed.

- Adopting the recommendations made in [45], to achieve an adequate use of real accelerograms in the nonlinear analysis of a multi-span bridge, ground motions may be amplified using a scale factor of 2.0.
- The interaction soil-structure is not taken into account and the ground is not modeled.
- Response in the inelastic interval is only evaluated for the RC column under study.
- Plastic hinges are placed at the ends of the column at 5% and 95% of the height.
- Springs are established at the beams' support ends and over the cap.
- Negligible second-order effects ($P - \Delta$).
- Neoprene bearing pads only work as a simply supported system.
- Fixed joints are included in the column bottom.
- The Hilbert Hughes Taylor integration method is employed.
- The Mander parametric approach is utilized for concrete modeling.
- The simultaneous presence of two vehicles with random weight and positions on the bridge is contemplated.

Figure 5 shows the FEM simplified model. It should be observed that some springs have been included not only in the support ends but also in the bent cap. This is to consider damping effects during the simulation exercise. After the detailing of the three categories of the framework, in the successive section the BN model will be proposed.

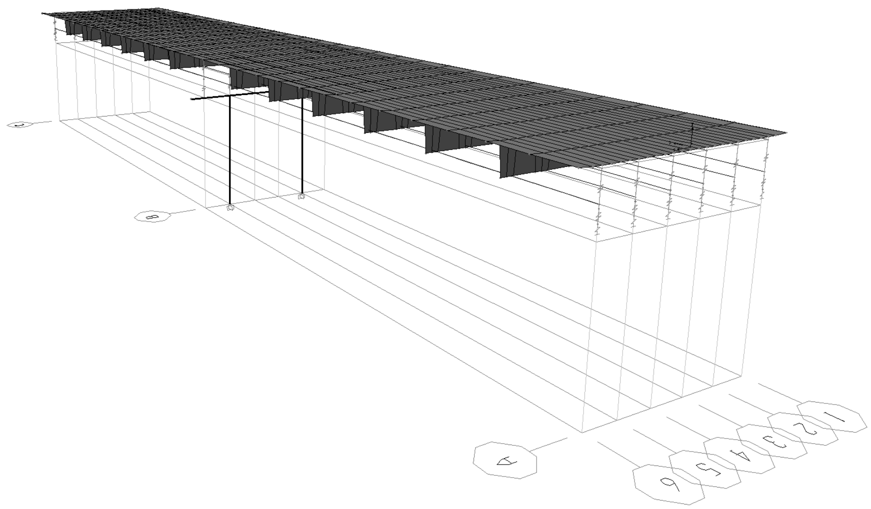

Figure 5: Simplified FEM model.

6. Bayesian network developed

The dependence structure of the data was modeled with a BN, that consists of 17 nodes (variables of interest) and more than 100 arcs illustrated in Figure 6. The model was built in the uncertainty analysis software package Uninet [46].

The occurrence of a seismic event of certain intensity (PGA) is independent of the vehicle weight in each lane of the bridge (WA1, WA2). The same is true for the number of axles in each lane (ApL1, ApL2) and the material properties ($f'c, Ec, fy, fu$). WA1 and WA2 in turn, are independent from one another. Similarly, the material properties of the concrete ($f'c, Ec$) are independent of the reinforcement steel strength (fy, fu). Moreover, ApL1 and ApL2 are conditionally independent of the force variables (MaxP, MaxV2, MaxV3, MaxM2, MaxM3) and the displacement variables (U1, U2, U3) given the loads on each section of the bridge (WA1, WA2).

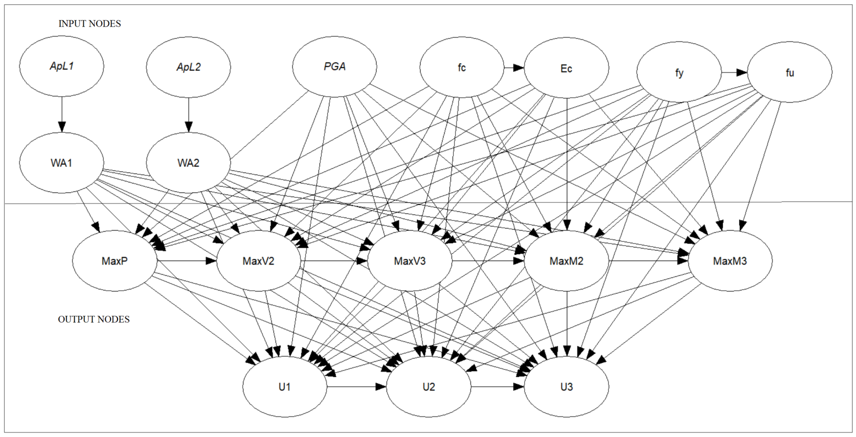

Figure 6: Proposed model.

The dependence between vehicles, earthquake intensity, material properties and force-displacement variables is complex. Hence, arcs from them to the remainder variables of the network are considered. The reason for this is that the BN model that would capture most of these interactions is precisely a complete graph (see the arrowheads converging in the output nodes in Figure 6). Once the graphical part of the model has been detailed, its validation process will be described.

6.1. Validation of the model

The dependence calibration score was estimated to validate the BN using Equation (4). Based on the approach exposed in [22] for calculating the d-score, a sample of 165 observations was generated 1800 times. This resulted in a d-score of 0.54, showing that the data has a normal copula (see Figure 7a ERC vs NRC). Similary, the resultant d-score between BNRC and NRC equals 0.868, demonstrating that the BN dependence is enough (see Figure 7b). This analysis concluded that the model was valid, hence valid reliability assessments can be carried out.

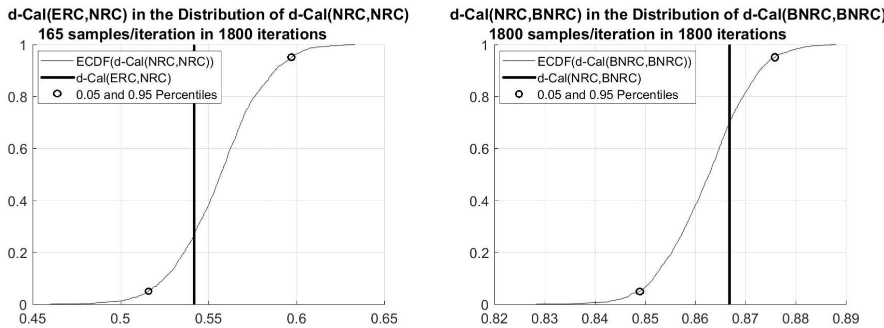

(a) The d-score of the ERC vs NRC

(b) The d-score of the BNRC vs NRC

Figure 7: Dependence calibration score.

7. Reliability analysis

The Oxford English Dictionary [47] defines reliability as *"the quality of being trustworthy or of performing consistently well"*. This definition is higly associated with the assessment of the POF [48]. To evaluate such a probability, a limit state function (Z) should be prior defined. In this case, Z is the condition beyond which, the structure or part of the structure does not longer fulfill one of its performance requirements. The limit state Z can be assessed by considering the resistance R and the loads L, i.e. $Z = L - R$. Failure occurs when $L > R$. Then, the probability of failure equals:

$$P_f = P(Z \geq 0) \tag{6}$$

As mentioned earlier, for the RC column analyzed, R will be estimated using the approach described in section 3. ln contrast, L will be obtained from the FEM analysis. Subsequently, the limit state functions required will be established.

7.1. Combined axial and flexural strength limit state function

The limit state function Z_{BC} is assessed by considering the position of the point (MaxM, MaxP) in the corresponding interaction diagram. The following two conditions are considered:

if the point is inside of the diagram area:

$$Z_{BC} = -1 * \sqrt{(MaxM - x_1)^2 + (MaxP - y_1)^2} \tag{7}$$

if the point is outside of the diagram area:

$$Z_{BC} = \sqrt{(MaxM - x_1)^2 + (MaxP - y_1)^2} \tag{8}$$

Where (x_1, y_1) are the coordinates of the closest point on the interaction diagram boundary to the point (MaxM, MaxP). Failure occurs when $Z_{BC} > 0$. Figure 8 shows two examples of the Z_{BC} value.

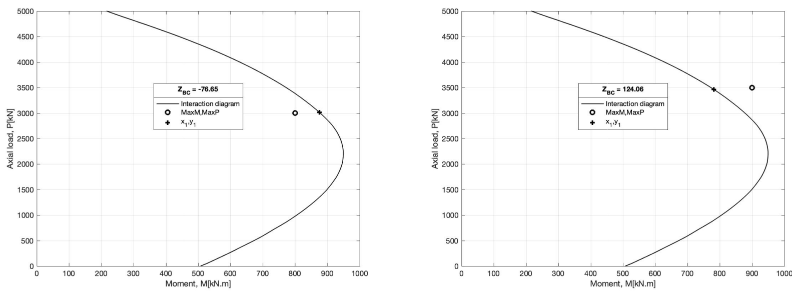

(a) (MaxM, MaxP) combination inside the interaction diagram, negative Z_{BC} value

(b) (MaxM, MaxP) combination outside the interaction diagram, positive Z_{BC} value

Figure 8: Z_{BC} value.

Therefore, the POF due to combined axial and flexural strength equals:

$$P_{fBC} = P(Z_{BC} \geq 0) \tag{9}$$

7.2. Shear strength limit state function

Here, the shear strength function Z_{Sh} is assessed by means of Vu, and the maximum acting shear in the element $(MaxV)$.

$$Z_{Sh} = MaxV - Vu \tag{10}$$

Thus, the POF due to shear (P_{fSh}) is:

$$P_{fSh} = P(Z_S h \geq 0) \tag{11}$$

7.3. Drift exceedance limit state function

Finally the drift exceedance function Z_γ is computed through γ and the maximum permissible drift γ_{max}.

$$Z_\gamma = \gamma - \gamma_{max} \tag{12}$$

The drift exceedance probability $(P_{f\gamma})$ is:

$$P_{f\gamma} = P(Z_\gamma \geq 0) \tag{13}$$

Once the model has been fully explained, its application will be presented in the next section, together with an analysis and discussion of its results.

8. Analysis and discussion

One of the advantages of the BN model, is that whenever evidence becomes available, the joint distribution may be updated accordingly. This procedure is referred to as conditionalization. Then, the BN is ready to be used for inference processes. It is also possible to condition either a unique value, or an interval.

In order to understand the use of the BN model, the instantiation process of the input nodes, using the PGA variable, will be illustrated. Making use of the intensities already presented in the last column of Table 1, they are firstly ranked from the minimum to the maximum value i.e. 0.00 to 1.026. Secondly, the 25th and 75th percentile values are calculated. In this case, they correspond to 0.273 and 0.783 respectively. Then, three ranges are proposed: (0.00,0.273) for low ground motion intensities; (0.273,0.783) for mid ground motion intensities; and (0.783,1.026) for high ground motion intensities.

The same steps are followed with the remainder selected input variables (WA1, WA2, $f'c, fy$). With this approach, 243 (3^5) scenarios can be analyzed. Each may help to determine the POF of the RC column subject to the combined action of, say, axial and flexural strength. Table 3 shows both the quantitative ranges found, and their qualitative labels.

Table 3: Input node labels.

Input node	LB	UB	Label
PGA[g]	0.000	0.273	Low
	0.273	0.783	Middle
	0.783	1.026	High
WA1[kN]	21.80	372.0	Low
	372.0	676.0	Middle
	676.0	1464.4	High
WA2[kN]	43.70	378.8	Low
	378.8	705.0	Middle
	705.0	1464.4	High
$f'c$[MPa]	22.70	30.00	Low
	30.00	34.80	Middle
	34.80	47.90	High
fy[MPa]	345.5	435.0	Low
	435.0	484.0	Middle
	484.0	619.7	High

To demonstrate the use of the BN in practice, an example is now provided. Suppose that the following scenario is randomly generated: PGA_{Middle}, $WA1_{High}$, $WA2_{High}$, $f'c_{Low}$, and fy_{Low}. Essentially, it represents a situation with considerable vehicle loads and low material resistances. Using a sample that satisfies the conditionalization of the five input variables, the limit state function (Z_{BC}) is evaluated. By means of an exceedance probability analysis [22], a POF=$3.35x10^{-7}$ is calculated. This probability is in line with the figures reported in [49], and corresponds to a small failure rate (lower than $1x10^{-6}$).

Figure 9 shows graphically the cumulative exceedance probability for this condition. While the dotted line represents the empirical distribution of Z_{BC}, the dashed one represents the corresponding extrapolation. As can be seen, the sample obtained from the conditionalized BN does not reach the failure state $Z_{BC} > 0$. In order to investigate the POF, the exceedance probability obtained from the BN may be extrapolated by usual probability distribution fitting techniques. These have been employed before, for example, in the context of bridge reliability using WIM data from the Netherlands in [50] and [51].

Seventeen continuous parametric distributions are fitted to the data through maximum likelihood estimation in MATLAB. The best fit is then selected based on Akaike's information criterion (AIC [52]). In the case of Figure 9, the result led to a t distribution with mean $\mu = -216.51$, scale parameter $\sigma = 27.773$ and shape parameter $\nu = 16.35$. Note that the t distribution approximates the Normal distribution as ν tends to infinity.

The data shown in Figure 9 is unimodal. For multimodal distributions in [50], [51] and [52] a finite mixture of Gaussian distributions is recommended in order to better represent tail behavior. Other POFs in table 4 have been computed by extrapolating the parametric distributions obtained from the BN, as judged by the AIC.

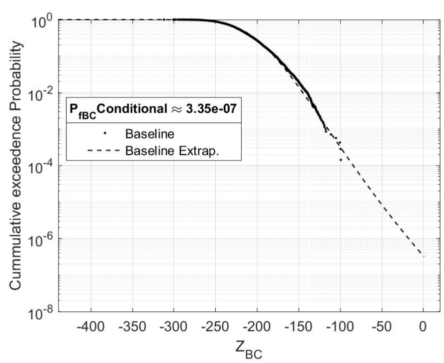

Figure 9: Conditional POF for the following case: PGA_{Middle}, $WA1_{High}$, $WA2_{High}$, $f'c_{Low}$, and fy_{Low}.

Given the large number of possible cases, 15 scenarios have been chosen for further analysis. The criteria for selection were as follows: one third of the events correspond to a low PGA, one third to a middle PGA and one third to a high PGA. For the loads ($WA1$ and $WA2$) and the resistances ($f'c$ and fy) there were 81 combinations. Although not exhaustive, five were used because they would give a general insight of the seeked probabilities. They are: (High-High, Low-Low), (Low-Low,Low-Low), (High-High, High-High), (Low-Low, High-High) and (Middle-Middle, Middle-Middle) respectively. Table 4 summarizes not only the described scenarios but also their associated probabilities of failure. Three POF's are being reported: P_{fBC}, P_{fSh} and $P_{f\gamma}$. Just as a reference, the β reliability index associated with the POFs found range from 3.1 to 8.1. [49].

Table 4: Probability of failures for each case

Cases	Peak Ground Acceleration (PGA)	Total weight per lane (WA)	Materials Resistance (f'c, fy)	P_{fBC}	P_{fSh}	$P_{f\gamma}$
	Level of conditionalization					
1	Low	High, High	Low, Low	2.24E-07	6.53E-04	3.62E-05
2		Low, Low	Low, Low	1.58E-07	9.46E-04	1.50E-05
3		High, High	High, High	1.11E-16	4.67E-11	2.99E-06
4		Low, Low	High, High	4.88E-15	1.33E-11	4.96E-06
5		Middle, Middle	Middle,Middle	3.33E-16	1.17E-08	6.10E-07
6	Middle	High, High	Low, Low	3.35E-07	1.28E-03	3.19E-04
7		Low, Low	Low, Low	2.17E-07	1.43E-04	1.64E-04
8		High, High	High, High	1.44E-14	7.49E-11	2.67E-05
9		Low, Low	High, High	3.57E-14	6.73E-11	2.63E-05
10		Middle, Middle	Middle, Middle	2.22E-16	7.61E-08	4.70E-05
11	High	High, High	Low, Low	1.09E-07	9.65E-04	4.17E-03
12		Low, Low	Low, Low	2.47E-07	5.39E-04	3.15E-03
13		High,High	High,High	1.11E-16	1.04E-11	4.32E-04
14		Low, Low	High,High	2.22E-16	6.37E-12	1.78E-04
15		Middle, Middle	Middle, Middle	1.45E-10	1.27E-07	1.32E-03

For the combined axial and flexural strength, the most adverse scenario is given by PGA_{Middle}, $WA1_{High}$, $WA2_{High}$, $f'c_{Low}$, and fy_{Low} (case 6) with a $P_{fBC} \approx 3.35x10^{-7}$. The next three are: case 12 with a $P_{fBC} \approx 2.47x10^{-7}$, case 7 with a $P_{fBC} \approx 2.17x10^{-7}$ and case 2 with a $P_{fBC} \approx 1.58x10^{-7}$. Once more, all of them are lower than $1x10^{-6}$, ratifying small failure rates [49]. It becomes apparent that the PGA has minimum influence in the P_{fBC}. However, it reveals the importance of the quality controls during the construction process, to avoid low material resistances.

In terms of the shear strength, case 6 represents the worst possible event with a $P_{fSh} \approx 1.28x10^{-3}$. This value corresponds to a large failure rate (close to $1x10^{-3}$) [49]. Now, for a middle PGA, the vehicle loads have an important influence in P_{fSh}, given low material resistances. It is worth noting that the P_{fSh} for case 7 is lower one order of magnitude than that for case 6. Moreover, it is lower eight orders of magnitude with respect to case 8 ($P_{fSh} \approx 7.49x10^{-11}$). This confirms the importance of quality controls to ensure high material resistances during the building stage.

Last but not least is the drift exceedance. Case 11 with a $P_{f\gamma} \approx 4.17x10^{-3}$ is now the most adverse scenario. This value is 1.3 times that of case 12 ($P_{f\gamma} \approx 3.15x10^{-3}$), meaning that the lower the vehicle loads, the lower the probability of failure. At this point, it was expected to obtain similar trends as those stated in [1]. Contrary to the finding reported here, they found a beneficial effect due to the presence of live loads. This was evidenced by the reduction of the measured displacements and probability of failure. In the same line of thought, more analyses may be performed. Those presented here have demonstrated the value of the proposed BN model. Finally, the main conclusions of this research will subsequently be drawn.

9. Conclusions

This document has dealt with concrete RC bridge columns and their acting loads and materials resistances. Having reviewed the literature, it became apparent that the combination of earthquake and live loads could lead to the failure of the structure under analysis. To better comprehend the bridge behavior, a probabilistic model was develop using the BN framework.

The proposed network includes the following variables: number of axles per lane, peak ground acceleration, total vehicle weight per lane, steel yield strength, tensile strength of the steel, compressive concrete strength, modulus of elasticity of the concrete, maximum axial load, maximum shear, maximum bending moment and displacements.

After quantifying all 17 variables by means of statistical historical data, in-situ tests and Monte Carlo simulations, their probability distributions were established. All of them were represented through empirical distributions, allowing the analyst to calculate the RC POF's.

At the outset, it was intended to include Mexican return periods in the bridge analysis. According to the civil construction manual of the federal electricity commission [53], the return period associated to the seismic demand, in the bridge location, ranges from 1000 to 2000 years. However, this recommendation was neglected since the Caltrans database was used to carry out the exercise. A similar decision was made with regard to the live load return period, which value is 50 years in the Mexican context [26], because the Dutch WIM data was utilized instead.

Having clarified this, the most adverse POF due to combined axial and flexural strength is approximately $3.35x10^{-7}$. The worst calculated POF due to shear force is approximately $1.28x10^{-3}$ and the most adverse for the maximum drift exceedance is approximately $4.17x10^{-3}$. Moreover, some scenarios can be simulated with the model. The results have the potential to help bridge managers in the resources allocation based on new available data.

Therefore, it is strongly believed that the methodology applied to build the model herein presented should serve as a reference. Basically, it might be applied to complete related exercises in different locations.

While the key objectives of this research have been achieved, there were a number of drawbacks associated with the work. Firstly, the limited availability of data records for quantifying the variables. Secondly, the use of in-situ tests has proven to be a time-consuming aspect for collecting information.

Overall, this research has demonstrated that the use of continuous probability distributions, generated through statistical data in concrete bridge columns, is not only reasonable but also advantageous. Even more, with new information the results can be updated through the proposed BN.

This work forms part of a bigger project aimed at developing a more comprehensive model applicable to the different components of a bridge. Finally, it is hoped that the results presented in this document are useful for the civil engineering community.

Acknowledgement

The authors would like to thank the Autonomous University of the State of Mexico (UAEMex) and the Mexican National Council for Science and Technology (CONACYT), for the financial support given through project UAEM 4322/2017/CI and scholarship CONACYT CVU 784544 to carry out this research. The authors also acknowledge Luis Horacio Martinez Martinez for their participation in the project.

References

[1] H. Wibowo, D. M. Sanford, I. G. Buckle, D. H. Sanders, The Effect Of Live Load On The Seismic Response Of Bridges, Technical Report, University of Nevada, Reno, 2013.

[2] J. Ghosh, C. C. Caprani, J. E. Padgett, Influence of traffic loading on the seismic reliability assessment of highway bridge structures, Journal of Bridge Engineering (2014).

[3] P. Tan, J. dong Huang, C.-M. Chang, Y. Zhang, Failure modes of a seismically isolated continuous girder bridge, Case Studies in Engineering Failure Analysis (2017).

[4] S. de Comunicaciones y Transportes, Sistema de puentes de méxico sipumex, 2009.

[5] S. S. N. de México, Catálogo de sismos, http://www2.ssn.unam.mx:8080/catalogo/, 2017.

[6] S. de Comunicaciones y Transportes, Datos viales, http://www.sct.gob.mx/carreteras/direccion-general-de-servicios-tecnicos/datos-viales/2018/, 2018.

[7] F. Seible, Visual Catalog of Reinforced Concrete Bridge Damage, Technical Report, California Department of Transportation, 2009.

[8] AASHTO (Ed.), AASHTO LRFD Bridge Design Specifications, American Association of State Highway and Transportation Officials (AASHTO), 2012.

[9] J. Wang, Bridge Engineering Handbook, Substructure Design, Piers and Columns, 2 ed., Taylor & Francis Group, 2014.

[10] J. K. Hsiao, Bending-axis effects on load-moment (p-m) interaction diagrams for circular concrete columns using a limited number of longitudinal reinforcing bars, Electronic Journal of Structural Engineering (2012).

[11] J.-H. Lee, S.-H. Ko, J.-H. Choi, Shear strength and capacity protection of rc bridge columns (2004).

[12] A. pública de la Ciudad de México, Normas técnicas complementarias para diseño y construcción de estructuras de concreto, 2017.

[13] M. L. Marsh, I. G. Buckle, E. Kavazanjian, LRFD Seismic analysis and design of bridges reference manual, Technical Report, U.S. Department of Transportation, 2014.

[14] A. pública de la Ciudad de México, Norma técnica complementaria para la revisión de la seguridad estructural de las edificaciones, 2017.

[15] Y.-M. Wang, T. Elhag, Fuzzy topsis method based on alpha level sets with an application to bridge risk assessment, Expert Systems with Applications 31 (2006) 309–319.

[16] Y. Wang, J. Liu, T. Elhag, L. Martinez, Bridge risk assessment using a hybrid ahp/dea methodology (2007).

[17] M. Billah, M. S. Alam, Seismic fragility assessment of highway bridges: a state-of-the-art review, Structure and Infrastructure Engineering 11 (2014).

[18] L. H. Martínez-Martínez, D. J. Delgado-Hernández, D. de León-Escobedo, J. Flores-Gomora, J. C. Arteaga-Arcos, Woody debris trapping phenomena evaluation in bridge piers: A bayesian perspective, Reliability Engineering System Safety 161 (2017) 38 – 52.

[19] J. Pearl, Probabilistic Reasoning in Intelligent Systems: Networks of Plausible Inference, Morgan Kaufmann Publishers Inc., San Francisco, CA, USA, 1988.

[20] C. Genest, J. Mackay, The joy of the copulas:biavariate distributions with uniform marginals, The American Statistician 40 (1986) 280–283.

[21] K. Pearson, Mathematical Contributions To The Theory Of Evolution.-XVI. On Further Methods Of Determinating Correlation, IV, Dulau, 1907.

[22] O. Morales-Nápoles, D. J. Delgado-Hernandez, D. D. Leon-Escobedo, J. C. Arteaga, A continuous bayesian network for earth dams' risk assessment: Methodology and quantification, Structure and Infrastructure Engineering (2014).

[23] R. Cooke, D. Kurowicka, Uncertainty Analysis With High Dimensional Dependence Modelling, 2006. doi:10.1002/0470863072.

[24] F. V. Jensen, Introduction to Bayesian Networks, 1st ed., Springer-Verlag, Berlin, Heidelberg, 1996.

[25] R. E. Neapolitan, Learning Bayesian Networks, Prentice-Hall, Inc., Upper Saddle River, NJ, USA, 2003.

[26] SCT, Nom-012-sct-2-2014, sobre el peso y dimensiones máximas con los que pueden circular los vehículos de autotransporte que transitan en las vías generales de comunicación de jurisdicción federal., 2014.

[27] S. Ferson, What monte carlo methods cannot do, Human and Ecological Risk Assessment: An International Journal 2 (1996) 990–1007.

[28] I. Díaz-Emparanza, Selection of the realizations number in a simulation study [in spanish], Estadistica Española 37 (1995) 497–509.

[29] A. García-Soto, A. Hernández-Martínez, J. Valdés-Vázquez, Probabilistic assessment of a design truck model and live load factor from weigh-in-motion data for mexican highway bridge design, Canadian Journal of Civil Engineering (2015).

[30] O. Morales-Nápoles, R. D. J. M. Steenbergen, Large-scale hybrid bayesian network for traffic load modeling from weigh-in-motion system data, Journal of Bridge Engineering (2015).

[31] J. Bommer, Strong motion parameters: definition, usefulness and predictability, in: 12 WCEE 2000 World Conference on Earthquake Engineering, 2000.

[32] J. E. Padgetts, B. G. Nielson, R. DesRoches, Selection of optimal intensity measures in probabilistic seismic demand models of highway bridge portfolios, Earthquake Engineering and Structural Dynamics (2007).

[33] B. de datos de registros acelerográficos de la red sísmica mexicana, Acelerográmas, http://aplicaciones.iingen.unam.mx/AcelerogramasRSM/Registro.aspx, 2018.

[34] I. nacional de electricidad y energías limpias, Programa de diseño sísmico (prodisis), https://www2.ineel.mx/prodisis/es/prodisis.php, 2017.

[35] A. Aviram, K. R. Mackie, B. Stojadinović, Guidelines for nonlinear analysis of bridge structures in California, 2008.

[36] K. R. Mackie, B. Stojadinović, Fragility Basis for California Highway Overpass Bridge Seismic Decision Making, Technical Report, Pacific Earthquake Engineering Research Center, 2005.

[37] ONNCCE, Nmx-c-161-onncce-2013, industria de la construcción - concreto fresco - muestreo., 2013.

[38] ONNCCE, Nmx-c-160-onncce-2004 industria de la construcción - concreto-elaboración y curado en obra de especímenes de concreto., 2004.

[39] ONNCCE, Nmx-c-109-onncce-2013 industria de la construcción - concreto hidráulico - cabeceo de especímenes, 2013.

[40] ONNCCE, Nmx-c-083-onncce-2014 industria de la construcción - concreto - determinación de la resistencia a la compresión de especimenes - método de ensayo, 2014.

[41] ONNCCE, Nmx-c-407-onncce-2001 industria de la construccín - varilla corrugada de acero proveniente de lingote y palanquilla para refuerzo de concreto - especificaciones y métodos de prueba, 2001.

[42] S. D. C. Y. F. INDUSTRIAL, Nmx-b-172-1988 métodos de prueba mecánicos para productos de acero, 1988.

[43] ONNCCE, Nmx-c-155-onncce-2014, industria de la construcción - concreto hidráulico - dosificación en masa - especificaciones y métodos de ensayo., 2014.

[44] E. Hernández, Sap2000 integrated software for structural analysis design. manual de aplicación del programa sap2000 v14, 2014.

[45] E. Kalkan, A. K. Chopra, Practical Guidelines to Select and Scale Earthquake Records for Nonlinear Response History Analysis of Structures, Technical Report, U.S. Geological Survey, 2010.

[46] S. Popinet, GTS: GNU Triangulated Surface library, `http://gts.sourceforge.net/`, 2000–2004.

[47] Oxford, English oxford dictionaries, https://en.oxforddictionaries.com/definition/reliability, 2018.

[48] M. Holicky, Reliability analysis for structural design, SUN MeDIA, Ryneveld Street, Stellenbosch, 7600, 2009.

[49] J. C. on Structural Safety, Probabilistic model code part 1 - basis of design, 2000.

[50] O. Morales-Nápoles, R. D.J.M.Steenbergena, Analysis of axle and vehicle load properties through bayesian networks based on weigh-in-motion data, Reliability Engineering and System Safety 125 (2014) 153 – 164.

[51] R. D.J.M.Steenbergena, O. Morales-Nápoles, Algemene veiligheidsbeschouwing en modellering van wegverkeerbelasting voor brugconstructies TNO-rapport, Technical Report, TNO, 2012.

[52] H. Akaike, A new look at the statistical model identification, IEEE Transactions on Automatic Control 19 (1974) 716–723.

[53] U. Mena-Hernández, A. Tena-Colunga, L. E. Pérez-Rocha, CAPITULO DE DISEÑO POR SISMO 2008. MANUAL DE DISEÑO DE OBRAS CIVILES DE CFE, Technical Report, Comisión federal de electricidad CFE, 2008.